Dye-sensitized Solar Cell Impedance Spectroscopy

Zurich Instruments

Application Note
Applications: photovoltaics, solar cells
Products: HF2LI, HF2LI-MF, HF2TA

Release date: April 2014

Summary

This application note gives an overview of the electrical impedance spectroscopy (EIS) technique used to characterize the photo-electrical performance of dye-sensitized solar cells (DSC) produced with different types of dye solutions. Since the interfaces within a solar cell can be modelled as an equivalent resistor and capacitor network, the electrical impedance spectroscopy technique can be applied to obtain the solar cell frequency response in the range from a few mHz all the way up to several MHz. Based on the measured response, one can then reconstruct the equivalent circuit model which can give qualitative insights into the efficiency of the DSC.

The HF2LI is a particularly well suited for EIS appliacations with its frequency range from DC to 50 MHz. The instruments' multi-frequency option enables users to obtain both amplitude and phase information at multiple arbitrary frequencies, including DC, at once. In addition, the dual synchronized input channels allow simultaneous measurement of the voltage drop and the through current in a DSC. These features make the HF2LI a very versatile, compact and flexible piece of instrument in solar cell impedance spectroscopy. The practical implementation of the HF2LI used for EIS is described. The presented results are based on a cooperation with the Department of Physics at the University of Basel [1].

Application

Today, most of the available photovoltaic modules containing silicon based solar cells suffer from a relatively high energy payback time [1]. Among the most efficient solar cells produced in research laboratories are the crystalline silicon based solar cells. Single junction crystalline silicon cells reach a maximal efficiency of approximately 25% [2] while the multi-junction cells can even reach 44% [4]. However, the aforementioned solar cells are unable to compete on a large scale with traditional carbon dioxide emission based energy sources due to the complex and expensive production processes. Hence, current solar cell research activities are driven by the need to find a cheap and more efficient alternative solar conversion technology. The dye-sensitized solar cell (DSC) discovered by Grätzel and O'Regan in 1991 [5] is one of the promising candidates. So far, DSCs have been integrated in devices achieving efficiencies above 12% with improved stability under outdoor conditions [6]. Moreover, under diffuse light conditions and at higher temperatures, they also perform relatively better compared to other solar cell technologies [7]. Additional advantages of DSCs are their large flexibility in shape, color and transparency, which opens up new integration possibilities in different applications [1].

In order to further improve DSC performance, the cells have to be analyzed by detecting and understanding the limitations to its photo-electrical performance. This is

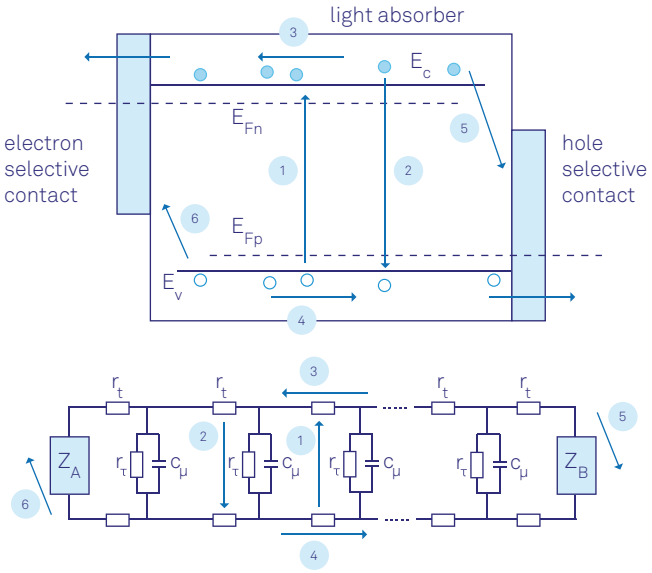

Figure 1. Top: DSC energy band diagram. Bottom: equivalent DSC diffusion model [1][10]

where electrical impedance spectroscopy (EIS) comes in. A small AC voltage is applied to the solar cell such that the cell's current and voltage response can be measured for each frequency of interest. The EIS technique is also widely used in material analysis for organic and hybrid solar cells [8]. Furthermore, EIS enables the comparison of solar cells to an equivalent circuit derived from theoretical calculations. The equivalent circuit, usually consisting of resistors and capacitors, is modelled based on the photoelectric and transport behavior determined by the structure and interfaces within a solar cell. By fitting the impedance measurement data to the equivalent circuit, one can gain insight into various interfaces determining the function and the efficiency of a solar cell. The next section will present the equivalent model for DSC solar cells.

DSC Transmission Line Model

Figure 1 illustrates how carriers transit between energy bands within a DSC. The movement can actually be modelled by a transmission line-type RC circuit. In addition, Z_A and Z_B are specific impedances describing charge transfer and recombination as well as polarization at the boundaries. If the distribution of the carriers is homogeneous inside the DSC, one can model the transmission line impedance $Z_{TL}(\omega)$ with the following equation [9]:

$$Z_{TL}(\omega) = \left(\frac{R_t R_\tau}{1+\frac{(i\omega)^\alpha}{\omega_\tau}}\right)^{0.5} \coth\left(\left[\frac{R_t}{R_\tau}\left(1+\frac{(i\omega)^\alpha}{\omega_\tau}\right)\right]^{0.5}\right)$$

R_t = total transport resistance in channel

R_τ = recombination resistance of nanoporous surface
$\omega_\tau = 1/(R_\tau C_\mu)$ = charge transfer frequency
α = model fitting parameter

The recombination resistance of the nanoporous solid is the most important parameter that indicates the performance of a solar cell. The higher the recombination resistance R_τ, the higher the fill factor [10]. A high fill factor means that the drop in current at a high voltage is delayed and therefore more electrons can be collected while the level of current is still close to the photocurrent (i.e. higher efficiency).

Beside the model for carrier transport behavior, one also needs to take into consideration the connection interface that is part of a complete DSC. A more complete diagram is shown in Figure 2. A simplified expression for the total impedance of a DSC is given below [11]:

$$Z_{total}(\omega) = R_s + \frac{1}{\frac{1}{Z_{TL}}(\omega) + \frac{1+i\omega R_{BL}C_{BL}}{R_{BL}}} + Z_d + \frac{R_{Pt}}{1+i\omega R_{Pt}C_{Pt}}$$

R_S = resistance of the conducting glass (TCO)
R_{BL} = back-layer resistance
C_{BL} = back-layer and electrolyte capacitance
Z_d = diffusion of the redox species in the electrolyte
R_{Pt} = charge transfer resistance
C_{Pt} = charge transfer capacitance

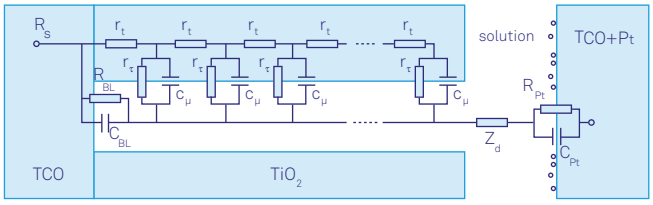

Figure 2. Complete DSC model with connection interfaces [10]

While $Z_{total}(\omega)$ is clearly a function of frequency, it also depends on the shunt potential V_p across the cell. In general, one can observe three different dominant impedance characteristics for low, medium and high potentials as shown in Table 1.

Table 1. Dominant DSC impedance element under different conditions

Shunt potential V_p	Dominant impedance
low	R_s, R_{BL}, C_{BL}, Z_d, R_{Pt}, C_{Pt}
intermediate	all
high	R_s, part of Z_{TL}, Z_d, R_{Pt}, C_{Pt}

V_{mpp} is the shunt voltage at which the solar cell generates the maximum power. The understanding of the fre-

quency and voltage dependence of the DSC impedance model now permits properly fitting the model parameters after the EIS measurement.

EIS Measurement Setup

Figure 3 shows the setup used for the DSC impedance measurement. The HF2LI Lock-in Amplifier has three functions:

- Bias solar cell shunt potential
- Measure I-V characteristic curve
- Electrical impedance spectroscopy: in this case, from 0.2 Hz to 100 kHz

The shunt potential is controlled through the Aux 1, one of the four HF2LI auxiliary outputs, which can generate ±10 V in 16-bit resolution. This DC bias is then added to the Add connector of one of the two 50 MHz sine wave generators. The resulting input excitation to the solar cell is then a sine wave with a DC offset. The second input of the HF2LI is used in differential mode (i.e. +In and -In Diff) to measure the shunt AC/DC voltage of the solar cell. On the output of the solar cell, an HF2TA current amplifier is used to measure the AC/DC current flowing through the solar cell by converting current into voltage. The output of the HF2TA amplifier is then measured by the input of the HF2LI.

In order to perform the frequency sweep, the ziControl graphical user interface can be used to control all settings of the HF2LI. Then, a frequency sweep can be easily performed which measures impedance $Z_{total}(\omega)$ over the desired frequency range. Note that the sub-Hz frequency range requires more digital filtering (i.e. longer integration time constant) in order to filter out 1/f noise of the measured signal. This may slow down the sweeper too much if measured over a wide frequency range. As a result, the sweep is performed in two steps: 0.2 Hz to 1 Hz and 1 Hz to 100 kHz. In the lower frequency range, the auto sinc filter function can be used in the sweeper which can help to reduce 1/f noise folding. Moreover, a short integration time constant can be used for the second high frequency range which allows a reduction of the overall measurement time.

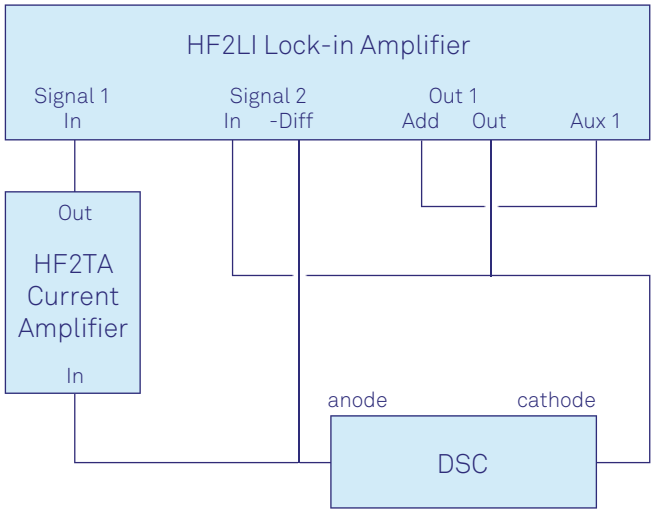

Figure 3. EIS measurement with HF2LI lock-in amplifier [1]

Model Fitting from EIS Measurement

The comparison has been performed on four dye solutions: crocetin, bixin, torularhodin and N719. These four DSCs were measured under illumination using the EIS technique. When applying approximately V_{mpp} to the four types of DSC, it was found that the fitting functions for intermediate voltages have to be used. Thus, all measurements were fitted with four fitting functions: Z_1, Z_2, Z_3 and Z_4 which were derived from the $Z_{total}(\omega)$ equation [10].

- Z_1 neglects diffusion ($Z_d = R_d = 0$) and uses the fitting parameter $\alpha = 1$
- Z_2 neglects diffusion and uses α as fitting parameter
- Z_3 is the same as Z_1 but takes diffusion into account (i.e. $Z_d \neq 0$)
- Z_4 is equal Z_3 but with α as fitting parameter and takes diffusion into account as well

The parameter α transforms the capacitance C_μ to a constant phase element CPE [8]. The CPE is used in the situation where a process has multiple dependencies as a function of frequency and therefore cannot be modelled properly with a capacitive element. The four different Z functions arising from this parameter were developed because, in certain cases, diffusion may be neglected at these voltages [1]. The least-square fits were done by Mathematica with FindFit which managed to find only local solutions.

The selection of the start values used for the fits was important to find the right solutions and were estimated by extracting the resistances from the Nyquist measurement directly. The width of the first semicircle corresponds to the charge transfer resistance R_{Pt} while the width of the second semicircle corresponds to the recombination resistance $R\tau$. Here we assume that the total transport resistance R_t must be smaller than the surface recombination resistance $R\tau$ in order for the material to be a good solar cell candidate. TCO glass resistance R_s can be extracted by the displacement of the semicircle from the origin of the fit. The maxima of the semicircles was extracted in the measurement data and C_μ and C_{Pt} were calculated respectively with:

$$C_\mu = 1/(2\pi f R_t)$$

$$C_{Pt} = 1/(2\pi f R_{Pt})$$

Result Interpretation

It was observed that there was a general phenomenon of drift when performing the DSC measurement. Take crocetin DSCs as an example, it was found that the chemical capacitance C_μ became smaller each time a measurement was taken. However, the value stayed around 250 µF. The drift was not very severe. Thus proper model extractions could be performed. For more details on why the measurement value drifts after each measurement please refer to [11].

For crocetin, the recombination resistance together with the chemical capacitance C_μ account for the large semicircle in the Nyquist plot. The back-layer resistance R_{BL} was found to be varying during the fitting process, even if the same start value was used. One must therefore be cautious when interpreting the extracted R_{BL} value. Fortunately, since it is a very large value, R_{BL} can be generally neglected. The value of the back-layer capacitance C_{BL} was extracted to be around 2 µF in all except the fitting function Z_3 where it also showed inconsistencies. Drift may also be the source of this inconsistency in the extracted C_{BL} value. More investigation would be required. R_{Pt} was estimated to be around 20 Ω and C_{Pt} around 12 µF. Both were very stable and were not influenced by the drift. R_{Pt} and C_{Pt} essentially determined the shape of the smaller semicircle at high frequencies, as shown in Figure 4. Note that the plot is traced from right (i.e. low frequencies) to left (i.e. high frequencies). More importantly, R_τ was found to be greater than R_t in crocetin which indicates low recombination. This gives a good indication that crocetin makes efficient DSCs.

The torularhodin DSC, on the other hand, is an example where the good solar characteristic was not fulfilled. One of the fit results is reproduced in Figure 5. The transport resistance R_t was found to be bigger than R_τ in most of the Z_1, Z_2, Z_3, Z_4 fitting results.

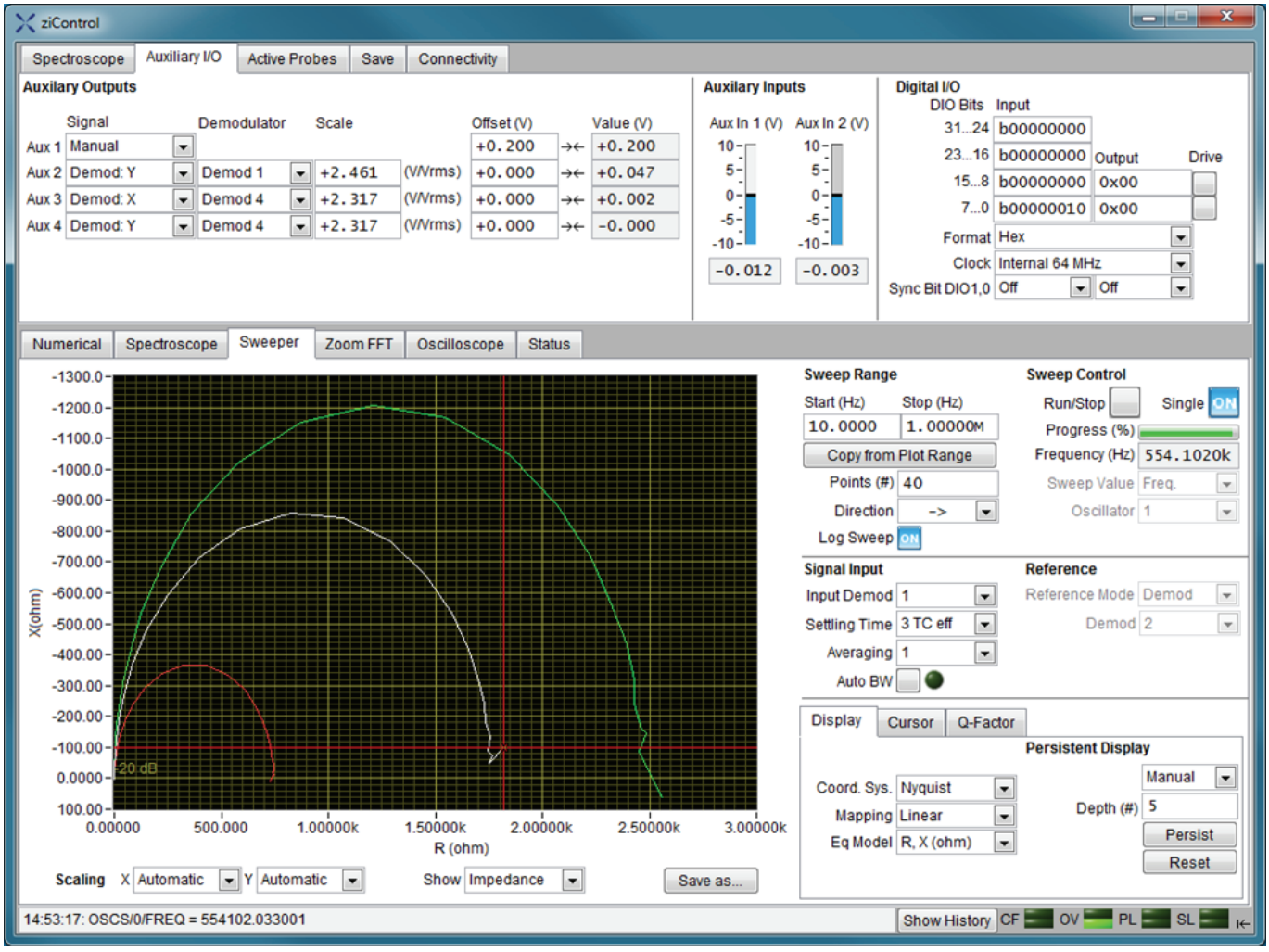

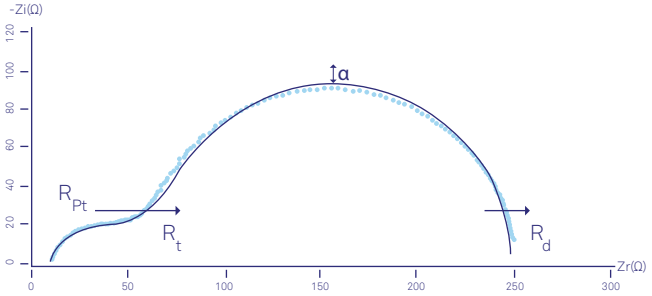

Figure 4. Fit of a Nyquist plot for crocetin DSC [1]

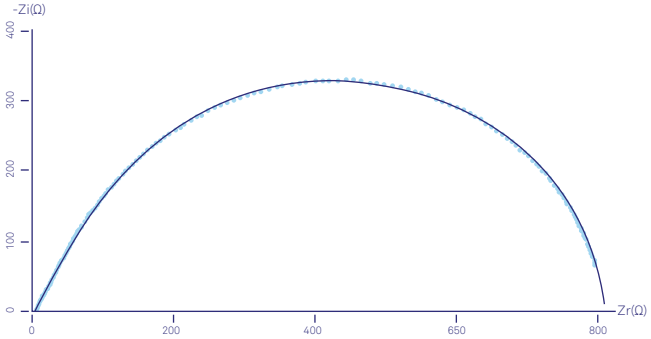

Figure 5. Fit of a Nyquist plot for torularhodin DSC [1]

Conclusions

Electrical impedance spectroscopy of four different dye-sensitized solar cells was performed using the HF2LI lock-in amplifier. The full integration in hardware and software allowed for both DC and AC impedance characterization to be performed on a very compact platform. Based on the measurement data, different model elements that represent the DSC diffusion behavior, the electrode interfaces as well as the internal interfaces were extracted using numerical fitting methods. EIS analysis and parameter extractions showed that the crocetin, bixin and N719 DSCs have low recombination which is essentially good for DSC efficiency. The torularhodin DSC, by contrast, has high recombination which makes it an non-ideal DSC candidate.

User Benefits

The Zurich Instruments HF2LI lock-in amplifier with HF2LI-MF option provides an powerful and flexible all-in-one platform for DSC power efficiency measurement and impedance spectroscopy:

- Dual channel input for simultaneous current and voltage measurement
- Frequency range from DC to 50 MHz
- Built-in frequency and parametric sweeper
- 6 arbitrary frequency demodulations including
- 4 auxiliary outputs for built-in DC biasing

Zurich Instruments also provides the HF2TA current amplifier that is connected to and fully controlled from the HF2LI without the need of an external power supply. The modular HF2TA can be placed close to the device-under-test while its output driver is 50 Ω which can be matched to the HF2LI input when the 50 Ω input impedance is selected.

Acknowledgements

Zurich Instruments would like to thank Jennifer Nussbaum and Dr. Thilo Glatzel from the University of Basel, Switzerland for their support and sharing application know-how and measurement results. We appreciate your involvement and continuous feedback.

References

[1] Nussbaum, J., Impedance Spectroscopy of Organic Dye-Sensitized Solar Cells, Project Thesis, Master of Science in Physics, University of Basel, May 14, 2013

[2] Jungbluth, N., Life Cycle Assessment of Crystalline Photovoltaics in the Swiss ecoinvent database. Progress in Photovoltaics: Research and Application, 13:429-446

[3] E. Martin A. Green, Keith Emery, Yoshihiro Hishikawa, Wilhelm Warta, and Ewan D. Dunlop. Solar cell efficiency tables (version 39). Prog. in Photovoltaics: Research and Applications, 20(1):1220, January 2012

[4] Science Daily, World Record Solar Cell With 44.7% Efficiency. September 23, 2013. Available at: http://www.sciencedaily.com/releases/2013/09/130923204214.htm

[5] Brian O'Regan and Michael Grätzel. A low-cost, high-efficiency solar cell based on dye-sensitized colloidal TiO2 films. Nature, 353(6346):737740, October 1991

[6] Aswani Yella, Hsuan-Wei Lee, Hoi Nok Tsao, Chenyi Yi, Aravind Kumar Chandiran, Md.Khaja Nazeeruddin, Eric Wei-Guang Diau, Chen-Yu Yeh, Shaik M Zakeeruddin, and Michael Grätzel. Porphyrin-sensitized solar cells with cobalt (ii/iii)-based redox electrolyte exceed 12 percent efficiency. Science, 334(6056):629634, November 2011

[7] Anders Hagfeldt, Gerrit Boschloo, Licheng Sun, Lars Kloo, and Henrik Pettersson. Dye-sensitized solar cells. Chem. Rev., 110(11):65956663, September 2010